Local position of Fe^{3+} in ferroelectric $BaTiO_3$

E. Siegel
Institut für Angewandte Physik, Universität Bonn, 5300 Bonn 1, West Germany

K. A. Müller
IBM Zurich Research Laboratory, 8803 Rüschlikon, Switzerland
and IBM Thomas J. Watson Research Center, Yorktown Heights, New York 10598

(Received 11 June 1979)

The EPR spectra of Fe^{3+} in the three ferroelectric phases of $BaTiO_3$ could be interpreted on the basis of the Newman superposition model. In the latter, the position of the nearest (oxygen) ligands determines the EPR spectrum. It is found that the Fe^{3+} participates by less than an order of magnitude in the collective motion of the Ti^{4+} ions out of their inversion symmetric position: by centering the Fe^{3+} and using previously determined intrinsic oxygen coordinates and parameters of the Newman model, the sign and magnitude of the EPR b_2^0 terms could be obtained for (a) the tegragonal phase, (b) the tetragonal ⟨001⟩ spectrum *perpendicular* to the ⟨110⟩ polarization in the orthorhombic phase, and (c) the very small ⟨111⟩ splitting in the rhombic phase; the electronic polarization being of the same magnitude in all three phases. The centered Fe^{3+} also yields correct EPR b_2^0 parameters for $PbTiO_3$ and $KNbO_3$. The investigation shows that the Fe^{3+} is a very sensitive probe of the intrinsic *oxygen positions*. The small coupling of the Fe^{3+} to the off-center ferroelectric motion is ascribed to its half-filled $3d$ shell.

I. INTRODUCTION

$BaTiO_3$ is one of the best-known displacive ferroelectric systems. It belongs to the perovskite structure and has three phase transitions, from cubic to tetragonal, tetragonal to orthorhombic, and orthorhombic to rhombohedral. The first complete study of Fe^{3+} in the tetragonal phase was carried out by Hornig, Rempel, and Weaver using c-domain crystals.[1] It was later compared to a similar study of Gd^{3+} by Rimai and de Mars.[2] Subsequent studies by Sakudo[3] and Sakudo and Unoki[4] extended the investigations to the orthorhombic $Amm2$ and rhombohedral $R3m$ phases. Domain selection was achieved by applying electric fields along the ⟨110⟩ and ⟨111⟩ cubic axes. The main results of these papers are:

(i) The local symmetry of Fe^{3+} in the cubic and tetragonal phases reflects the symmetry of the bulk material.[1] The $b_2^0(T)$ parameter is positive, large, and proportional to the square of the polarization, $[P(T)]^2$.[2]

(ii) In the orthorhombic phase, the EPR spectrum does not show the orthorhombicity of the bulk material. The local symmetry is tetragonal, with its axis parallel to a cubic ⟨100⟩ axis *perpendicular* to the spontaneous ⟨110⟩ polarization. The $b_2^0(T)$ splitting is half as large as in the tetragonal phase but *negative*.[3]

(iii) In the rhombohedral phase, the axial splitting parameter b_2^0 was found to be more than an order of magnitude smaller than in the orthorhombic and tetragonal phases; contrary to expectations, since in all three phases the spontaneous Ti displacement and the polarizations are of the same order of magnitude.[3,4]

(iv) The cubic parameter a is nearly insensitive to the phase transitions.[1–4]

On the other hand Takeda[5] extended the EPR research of Gd^{3+} to the lower two phases of $BaTiO_3$. He reported axial $|b_2^0|$ terms directed along ⟨110⟩ and ⟨111⟩ axes of almost the same magnitude of 267×10^{-4} and 340×10^{-4} cm^{-1}, respectively, as compared to 294×10^{-4} cm^{-1}, in the tetragonal phase. Thus the b_2^0 values of Gd^{3+} are perfectly normal in their direction and magnitude to the observed polarizations in the three phases.

The aim of this paper is to give an understanding of the unexpected behavior of Fe^{3+} in $BaTiO_3$, which has not been clarified till now. The analytic basis of this understanding is the superposition model of Newman[6] reviewed by Newman and Urban.[7] Owing to the latest success of this model in the interpretation of the Fe^{3+} EPR data, it is now possible to obtain detailed information on the local surroundings of the Fe^{3+} ion as demonstrated by Siegel and Müller.[8]

Up to now, in the interpretation of the Fe^{3+} EPR parameters in $BaTiO_3$ two assumptions have been made, first the Fe^{3+} is on the Ti^{4+} site, and second, the Fe^{3+} has ionic coordinates identical to Ti^{4+}. These assumptions are the natural basis for EPR experiments from which information on the bulk ma-

terial would be desirable by doping with a paramagnetic ion. The first assumption can be shown to be fulfilled in $BaTiO_3$ by comparing its cubic parameter a with that of MgO or $SrTiO_3$, where it is known that Fe^{3+} has a sixfold oxygen coordination.[8,9] The second assumption originated from properties (i) in the tetragonal phase, which will be shown not to hold. From the present calculations the information is derived that Fe^{3+} is located in the center of the octahedron, and does not follow the Ti^{4+} motion which is displaced by about 0.1 Å from the center. The Fe^{3+} EPR parameters are *very sensitive probes* of the *intrinsic* oxygen positions. With this knowledge the open questions cited above including properties (i) can be explained. Furthermore, it will be shown that the same model yields correct b_2^m parameters for Fe^{3+} in $PbTiO_3$ and $KNbO_3$. The available data on Mn^{2+} indicate the same behavior.

II. MODEL CALCULATION FOR Fe^{3+} IN THE THREE FERROELECTRIC PHASES OF $BaTiO_3$

The present interpretation of the unexpected behavior of Fe^{3+} in $BaTiO_3$ is based on the Newman superposition model. We have reviewed this model for Fe^{3+} in Ref. 8. The essential equation, which correlates the EPR parameters b_2^0 and b_2^2 with the surroundings of the paramagnetic ion is

$$b_2^m = \bar{b}_2(R_0) \sum_{i=1}^{N} \left(\frac{R_0}{R_i}\right)^{t_2} K_2^m(\theta_i, \psi_i) \quad . \tag{1}$$

In this equation the various symbols have the following meanings: R_i are the distances between the paramagnetic ion Fe^{3+} and the ligand ion i. R_0 is the reference point, normally chosen near a value of the R_i's. θ_i is the angle between the EPR main axis, the Fe^{3+} ion, and ligand ion i. ψ_i is the angle between the EPR x axis and the projection of the ligand coordinates of ion i in the x-y plane. N is the coordination number.

$$K_2^0(\theta) = \tfrac{1}{2}(3\cos^2\theta - 1) \quad ,$$

$$K_2^2(\theta, \psi) = \tfrac{3}{2}\sin^2\theta\cos 2\psi \quad ,$$

and $\bar{b}_2(R_0)$ is the intrinsic parameter. For Fe^{3+} as paramagnetic ion this parameter $\bar{b}_2(R_0)$ can be obtained from the distance dependence of Eq. (2) derived from MgO,[8,10]

$$\bar{b}_2(R_0) = \bar{b}_2(2.101\ \text{Å})\left[\frac{2.101\ (\text{Å})}{R_0\ (\text{Å})}\right]^{t_2} \quad , \tag{2}$$

with $\bar{b}_2(2.101\ \text{Å}) = -0.412(25)\ \text{cm}^{-1}$ and the power-law exponent $t_2 = 8(1)$.

A. Substitutional Fe^{3+} with Ti^{4+} coordinates

In this model we assume that Fe^{3+} is on the Ti^{4+} site with ionic coordinates identical to Ti^{4+}. This model corresponds to the assumptions normally made in EPR. The local surroundings of Fe^{3+} consist of an oxygen octahedron distorted in the tetragonal, orthorhombic, and rhombohedral phases. For the three ferroelectric phases of $BaTiO_3$ the coordinates of the ions are given in Figs. 1–3 using the data of Refs. 11–14. The site of the Ti^{4+} and Fe^{3+} ion was chosen as the origin of the coordinate system ($\Delta \equiv 0$). With the ionic coordinates given in the three figures and the crystallographic data of Table I, b_2^0 and b_2^2 could be calculated using Eq. (1). The results for the three phases of $BaTiO_3$ are given in Table II, where the experimental values are shown in the first column. In the second, the calculated values for the Ti coordinate model are presented. A comparison shows that three fundamental discrepancies exist. (i) The calculated signs of b_2^0 in the tetragonal, orthorhombic, and rhombohedral phases are opposite to the measured signs. (ii) The calculated value of b_2^2 in the orthorhombic phase is large, whereas the measured value of b_2^2 is zero within the experimental-error limit. (iii) In the rhombohedral phase, the calculated value shows a strong axiality compar-

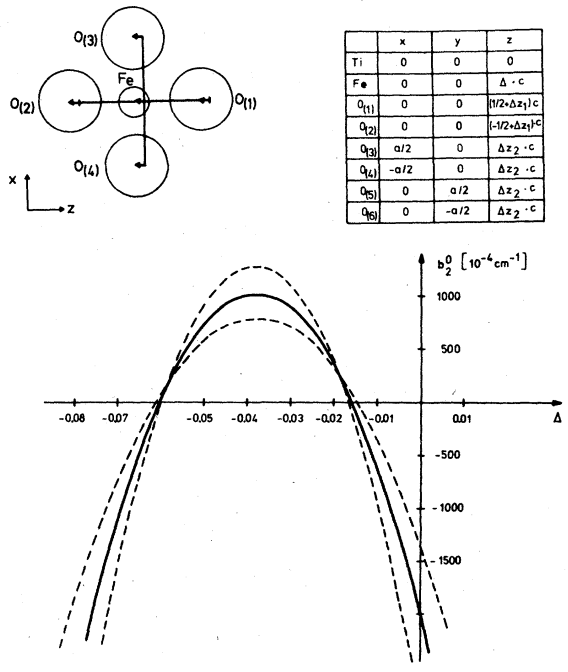

	x	y	z
Ti	0	0	0
Fe	0	0	Δ·c
$O_{(1)}$	0	0	(1/2+Δz$_1$)c
$O_{(2)}$	0	0	(-1/2+Δz$_1$)c
$O_{(3)}$	a/2	0	Δz$_2$·c
$O_{(4)}$	-a/2	0	Δz$_2$·c
$O_{(5)}$	0	a/2	Δz$_2$·c
$O_{(6)}$	0	-a/2	Δz$_2$·c

FIG. 1. Local environment, the coordinates of the ions and the computed value of b_2^0 for Fe^{3+} in the tetragonal phase of $BaTiO_3$. In the environment, the signs of the intrinsic oxygen shifts for $BaTiO_3$ are included.

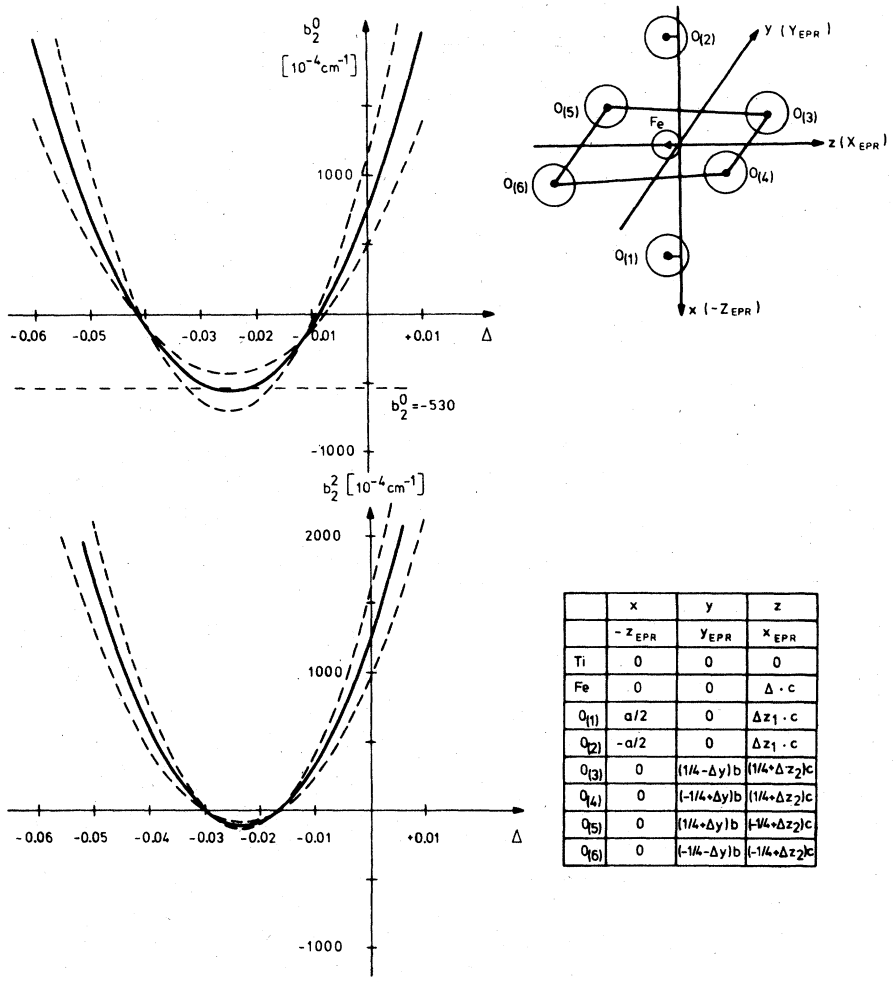

	x	y	z
	$-z_{EPR}$	y_{EPR}	x_{EPR}
Ti	0	0	0
Fe	0	0	Δ · c
$O_{(1)}$	a/2	0	$\Delta z_1 \cdot c$
$O_{(2)}$	-a/2	0	$\Delta z_1 \cdot c$
$O_{(3)}$	0	(1/4-Δy)b	(1/4+Δz_2)c
$O_{(4)}$	0	(-1/4+Δy)b	(1/4+Δz_2)c
$O_{(5)}$	0	(1/4+Δy)b	(-1/4+Δz_2)c
$O_{(6)}$	0	(-1/4-Δy)b	(-1/4+Δz_2)c

FIG. 2. Local environment, with the signs of the oxygen shifts included, the coordination of the ions and the prediction for b_2^0 and b_2^2 in orthorhombic $BaTiO_3$.

able to the tetragonal and orthorhombic phases, which is not found experimentally. From these three discrepancies, we conclude that Fe^{3+} does not have ionic coordinates identical to Ti^{4+}. Thus Fe^{3+} behaves differently from Ti^{4+}. The other alternative would be that the superposition model is incorrect; however, this can be excluded by the success of the model in the interpretation of Fe^{3+} data in our previous paper.[8] The validity of this model for Fe^{3+} and Gd^{3+} ions regarding the b_2^m parameters has also been confirmed more recently by Buzaré.[15]

B. One-parameter model

In the substitutional model we obtained the result that Fe^{3+} cannot be sited on intrinsic Ti^{4+} coordinates. In the one-parameter model, we therefore assume that Fe^{3+} deviates from the exact crystallographic position. This deviation is described by a displacement Δ, which is parametrized in units of the lattice constants. The displacement is assumed to be in the direction of the polarization in each phase. For a given value of Δ the distances and angles were calculated and with Eq. (1), b_2^0 and b_2^2 were determined. The result of this calculation is shown in Figs. 1–3. The full lines represent the predictions of b_2^0 or b_2^2 for $t_2=8$ and the calculated value of $\bar{b}_2$, using Eq. (2). The dashed curves demonstrate the range of uncertainty emanating from the errors of t_2 and $\bar{b}_2$. For zero displacement $\Delta=0$, Fe^{3+} is located on the exact Ti^{4+} position; therefore this one-parameter model includes the substitutional model discussed above.

For the tetragonal phase of $BaTiO_3$ (Fig. 1) it can be seen that positive values of b_2^0 can be obtained. For a displacement parameter $\Delta=-0.032$, the experimental value of $b_2^0=+929\times10^{-4}$ cm^{-1} can be explained. Including the errors in $\bar{b}_2$ and t_2, using

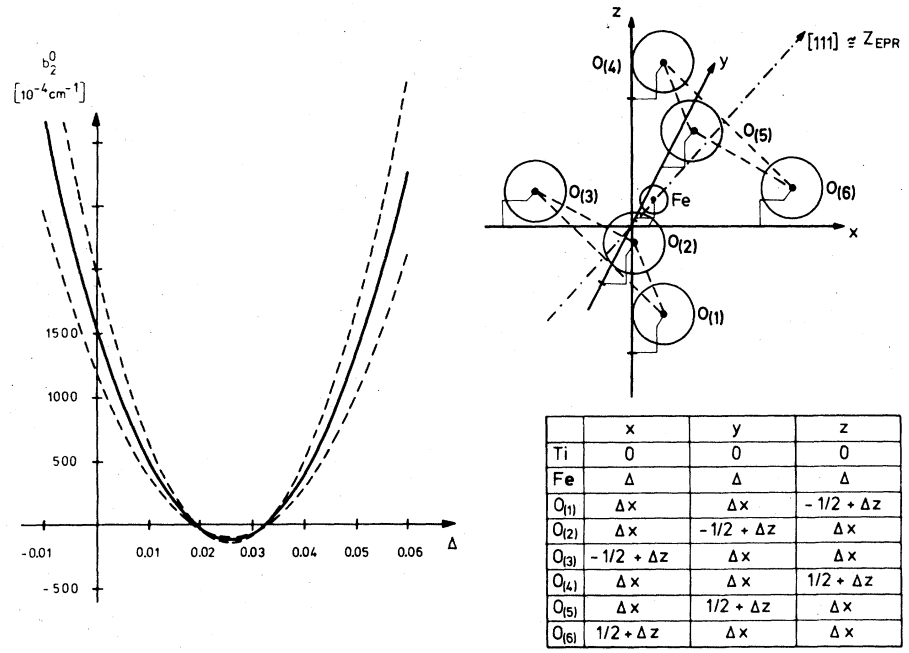

	x	y	z
Ti	0	0	0
Fe	Δ	Δ	Δ
$O_{(1)}$	Δx	Δx	-1/2 + Δz
$O_{(2)}$	Δx	-1/2 + Δz	Δx
$O_{(3)}$	-1/2 + Δz	Δx	Δx
$O_{(4)}$	Δx	Δx	1/2 + Δz
$O_{(5)}$	Δx	1/2 + Δz	Δx
$O_{(6)}$	1/2 + Δz	Δx	Δx

FIG. 3. Local environment, the coordination of the ions in the rhombohedral system and the computed b_2^0 for this structure.

$\Delta \leq -0.027$, the sign and the magnitude of b_2^0 can also be obtained.

In the orthorhombic phase, b_2^0 and also $b_2^2 \approx 0$ had to be explained. In Fig. 2 the prediction of the one-parameter model is shown. The sign and the amount of the measured b_2^0 can be obtained for $\Delta = -0.022$. Taking the errors of t_2 and $\bar{b}_2$ into account, values of $\Delta \leq -0.018$ are also possible to obtain the experimental value of b_2^0. The Δ range from −0.018 to −0.022 also yields simultaneously the very low value of b_2^2. To obtain $b_2^2 = 0$, $\Delta = -0.017$ had to be used.

In the rhombohedral phase, Fig. 3, it can be seen that negative values of b_2^0 are only obtainable in a small Δ range. To get $b_2^0 = -23 \times 10^{-4}$ cm^{-1}, a value of $\Delta = +0.02$ had to be taken.

By this one-parameter model, which only varies the Fe^{3+} position and takes the oxygens on the ideal crystallographic position, *all* measured amounts and signs of b_2^0 or b_2^2 in $BaTiO_3$ can be explained for one specific chosen value of Δ in each phase summarized

TABLE I. Superposition-model parameters, lattice constants, and oxygen shift data for the tetragonal, orthorhombic, and rhombohedral phases of $BaTiO_3$.

$BaTiO_3$	Tetragonal phase	Orthorhombic phase	Rhombohedral phase
Superposition-model data	$R_0 = \frac{1}{2}c = 2.018$ Å	$R_0 = \frac{1}{2}a = 1.995$ Å	$R_0 = R_{cub} = 1.998$ Å
	$\bar{b}_2(R_0) = -0.569(62)$ (cm^{-1})	$\bar{b}_2(R_0) = -0.623(75)$ (cm^{-1})	$\bar{b}_2(R_0) = -0.616(73)$ (cm^{-1})
	$t_2 = 8(1)$	$t_2 = 8(1)$	$t_2 = 8(1)$
Lattice constants	$a = b = 3.9920$ Å $c = 4.0361$ Å	$a = 3.990$ Å $b = 5.669$ Å $c = 5.862$ Å	$a = b = c = 4.004$ Å $\alpha = \beta = \gamma = 89.87$ Å
	at $T = 293$ K, Ref. 11	at $T = 263$ K, Ref. 13	at $T = 132$ K, Ref. 14
Oxygen shift data	$\Delta z_1 = -0.0398(10)$ $\Delta z_2 = -0.0303(10)$	$\Delta z_1 = -0.020$ $\Delta z_2 = -0.023$ $\Delta y = +0.003$	$\Delta x = 0.0221(5)$ $\Delta z = 0.0291(4)$
	at $T = 300$ K, Ref. 12	at $T = 274$ K, Ref. 13	at $T = 132$ K, Ref. 14

TABLE II. Comparison of the experimental Fe^{3+} EPR data with three different models on the basis of the superposition model.

	Experimental EPR data (10^{-4} cm^{-1})	Ti coordinate model (10^{-4} cm^{-1})	One-parameter model; deviation Δ to obtain the experimental EPR value		Centered model (10^{-4} cm^{-1})
Tetragonal phase	$b_2^0 = +929$ at $T = 300$ K, Ref. 1	$b_2^0 = -2028(700)$	$\Delta \approx -0.03$	$D = \Delta \times c$ $= -0.12$ Å	$b_2^0 = +1047(250)$
Orthorhombic[a] phase	$b_2^0 = -530(10)$ $b_2^2 = 0$ at $T = 276$ K, Ref. 2	$b_2^0 = +760(300)$ $b_2^2 = +1245(300)$	$\Delta \approx -0.02$	$D = \Delta \times c$ $= -0.11$ Å	$b_2^0 = -565(136)$ $b_2^2 = -82(22)$
Rhombohedral phase	$b_2^0 = -23(5)$ at $T = 173$ K, Ref. 4	$b_2^0 = +1585(400)$	$\Delta \approx +0.02$	$D = \Delta\sqrt{3} \times a$ $= 0.14$ Å D along [111]	$b_2^0 = -83(19)$

[a]EPR main axis along a ⟨100⟩ axis.

in Table II. Comparing the Δ values of Table II with the crystallographic oxygen shift data of Table I in the tetragonal, orthorhombic, and rhombohedral phases, the signs of both values are the same. The amounts of the shift data and the displacive parameter are also quite similar. This means that the Fe^{3+} has about the same deviation from the ideal crystallographic Ti^{4+} position as the shift of the oxygens in all phases of $BaTiO_3$ through any of their phase transitions. Therefore Fe^{3+} is sited near the center of the octahedron. Considering now that the octahedron is immobile, then the Ti^{4+} ion is at the center of the octahedron in the cubic phase, and shifts off-center by about 0.1 Å along the ⟨100⟩, ⟨110⟩, or ⟨111⟩ directions in the tetragonal, orthorhombic, and rhombohedral phases. However, Fe^{3+} remains, according to our results, in all phases near the center of the octahedron.

C. Centered model

From the one-parameter model, we have learned that the experimental EPR values can be explained if we assume that Fe^{3+} is near the center of the octahedron. We take this result as the starting point in the centered model which assumes: (i) Fe^{3+} is at the center of the octahedron. (ii) The distortions in the oxygen octahedron surrounding Fe^{3+} will be caused only through changes in the lattice constants. In Fig. 4 the octahedrons are drawn for all four phases of $BaTiO_3$. This figure also includes the superposition-model equations for this specific model. Inserting the crystallographic data of Table I, the EPR parameters in Table II of the last column are obtained.

The calculated sign of b_2^0 is identical with the measured sign in all three ferroelectric phases. The amounts of b_2^0 in the tetragonal and orthorhombic phases can be predicted very well. The parameter b_2^2 in this model originates only from the differences in the lattice constants b and c. If b were equal to c, b_2^2 would be zero and a fourfold symmetry axis with a cubic axis as the EPR main axis would be obtained. The calculated value of b_2^2 is very small compared to

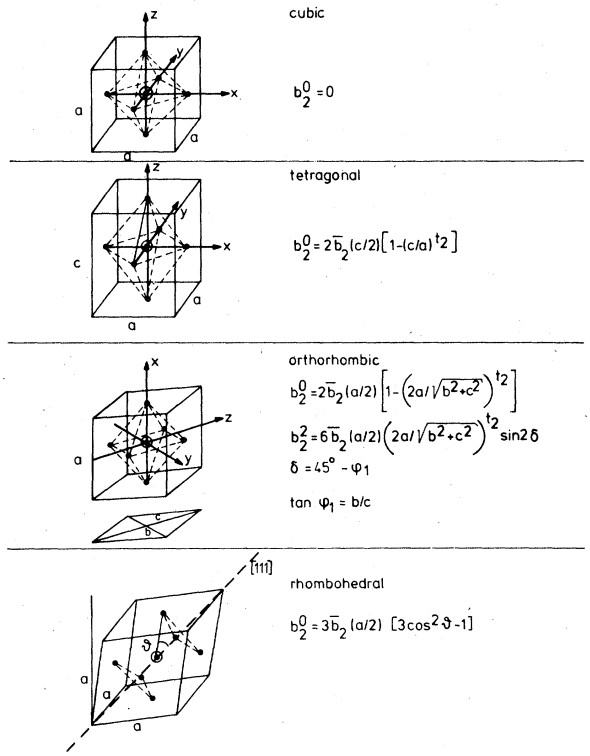

FIG. 4. Superposition-model equation for the centered model in the four phases of $BaTiO_3$.

that of the Ti coordinate model. The error of b_2^2 given in Table II originated only from the error in the lattice constants and from the error in $\bar{b}_2$.

In the rhombohedral phase, the parameter b_2^0 is 20 times smaller than in the Ti coordinate model. It also has the correct order of magnitude. The absolute value is somewhat larger than the measured value. The error given here comes from the assumed error in the rhombohedral angle γ of 0.02° and that of $\bar{b}_2$. The main result of this model is that all the experimental b_2^0, b_2^2 data of $BaTiO_3$ can be explained sufficiently in centering the Fe^{3+} and taking the intrinsic oxygen coordinates.

III. Fe^{3+} IN TETRAGONAL $PbTiO_3$ AND ORTHORHOMBIC $KNbO_3$

There are only a few oxide perovskites, apart from $BaTiO_3$ and $SrTiO_3$, with known Fe^{3+} EPR data. Therefore, with the same models as for $BaTiO_3$, the $PbTiO_3$ and $KNbO_3$ compounds were investigated, and in Table III, all relevant data for these two compounds are given, i.e., the crystallographic and those on Fe^{3+} EPR in $PbTiO_3$ (Refs. 16 and 17) and $KNbO_3$ (Refs. 18 and 19), respectively.

The remarkable features of tetragonal $PbTiO_3$ are: The Ti coordinate model predicts the wrong sign of b_2^0; therefore Fe^{3+} has ionic coordinates different from Ti^{4+}. On the other hand, the centered model correctly predicts the sign and magnitude of the experimental EPR data. Therefore Fe^{3+} in $PbTiO_3$ behaves in the same manner as Fe^{3+} in $BaTiO_3$.

For $KNbO_3$, only EPR data for the orthorhombic phase are known without the knowledge of the signs of b_2^0 and b_2^2. From a comparison with the orthorhombic phase of $BaTiO_3$, one would expect a negative sign of b_2^0. In the Nb coordinate model, the calculated b_2^2 parameter is an order of magnitude too large; therefore the ratio b_2^2/b_2^0 is also too large compared with the experimental value. Hence Fe^{3+} again behaves differently from Nb^{5+}. In the centered model, the value of b_2^0 and also the correct order of magnitude of b_2^2 can be successfully predicted.

The calculated value of b_2^2 is too small, perhaps due to the too simple assumption about the oxygen surroundings. These two compounds show that the behavior of Fe^{3+} in $BaTiO_3$ is not an exception but rather a more common feature than expected.

TABLE III. Results of the model calculations for Fe^{3+} in tetragonal $PbTiO_3$ and orthorhombic $KNbO_3$.

	Fe^{3+} in tetragonal $PbTiO_3$	Fe^{3+} in orthorhombic $KNbO_3$
Superposition-model data	$R_0=\frac{1}{2}c=2.076$ Å	$R_0=\frac{1}{2}a=1.986$ Å
	$\bar{b}_2(R_0)=-0.453(36)$ (cm^{-1})	$\bar{b}_2(R_0)=-0.646(81)$ (cm^{-1})
	$t_2=8(1)$	$t_2=8(1)$
Lattice constants	$a=3.904$ Å	$a=3.973$ Å
	$c=4.152$ Å	$b=5.695$ Å
		$c=5.721$ Å
	at $T=300$ K, Ref. 16	at $T=195$ K, Ref. 18
Oxygen shift data	$\Delta z_1=1.072$	$\Delta z_1=0.0375$
	$\Delta z_2=2.072$	$\Delta z_2=0.0336$
		$\Delta y=-0.0011$
	at $T=300$ K, Ref. 16	at $T=195$ K, Ref. 18
Experimental EPR data	$b_2^0=+5300(200)10^{-4}$ cm^{-1}	$\lvert b_2^0\rvert=1776(1)10^{-4}$ cm^{-1}
		$\lvert b_2^2\rvert=293(3)10^{-4}$ cm^{-1}
		$\lvert b_2^2/b_2^0\rvert=0.165(2)$
	at $T=290$ K, Ref. 17	at $T=300$ K, Ref. 19
Ti and Nb coordinate model	$b_2^0=-4676(2000)10^{-4}$ cm^{-1}	$b_2^0=1105(470)10^{-4}$ cm^{-1}
		$b_2^2=2572(650)10^{-4}$ cm^{-1}
		$b_2^2/b_2^0=2.3\pm1.6$
Centered model	$b_2^0=+5774(1400)10^{-4}$ cm^{-1}	$b_2^0=-1525(370)10^{-4}$ cm^{-1}
		$b_2^2=-155(34)10^{-4}$ cm^{-1}
		$b_2^2/b_2^0=0.10(5)$

IV. Mn^{2+} IN TETRAGONAL $BaTiO_3$ AND $PbTiO_3$

In Secs. I–III we saw that Fe^{3+} behaves differently from Ti^{4+}. To see whether the paramagnetic ion Fe^{3+} is an exception, we looked at the behavior of Mn^{2+} in ferroelectric oxide perovskites and also analyzed the Mn^{2+} EPR data of tetragonal $BaTiO_3$ and $PbTiO_3$.

The basis of the analysis is also the superposition model with the intrinsic $\bar{b}_2(R)$ function for Mn^{2+} with oxygen as ligand derived from MgO in Ref. 10. The functional dependence is given in Eq. (3)

$$\bar{b}_2(R) = \bar{b}_2(2.101\ \text{Å}) \left[\frac{2.101\ (\text{Å})}{(\text{Å})} \right]^{t_2}, \qquad (3)$$

with $\bar{b}_2(2.101\ \text{Å}) = -0.1575(5)\ \text{cm}^{-1}$ and $t_2 = 7(1)$.

The EPR data for $BaTiO_3$ and $PbTiO_3$ were taken from Refs. 20 and 21, respectively. The site determinations of Mn^{2+} for $BaTiO_3$ were done in Ref. 8. With the crystallographic data of Refs. 11 and 12 (Table I) and that of Ref. 16 (Table III), for the three models we obtain the data of Table IV.

For both compounds, the Ti coordinate model predicts the wrong sign of b_2^0. Therefore we must conclude that Mn^{2+} also has ionic coordinates different from those of Ti^{4+}. The one-parameter model shows that Mn^{2+} tends to move towards the center of the octahedron but it is not located in the center, like the centered model, as also shown by the displacement parameter Δ. The main characteristics are: (i) Mn^{2+} does not have identical coordinates like Ti^{4+} in these ferroelectric oxide perovskites either; (ii) the directions of the displacement of the Fe^{3+} and Mn^{2+} ions are the same; and (iii) the positions of Fe^{3+} and Mn^{2+} are different in these compounds probably due to the difference in the nominal charge and the sizable difference in the ionic radii $[r(Mn^{2+}) - r(Ti^{4+}) = 0.23\ \text{Å}]$.[22]

V. DISCUSSION

The superposition model shows that Fe^{3+} in ferroelectric $BaTiO_3$ does not have ionic coordinates identical to Ti^{4+}. It is in the center of the octahedron. The Fe^{3+} ion, therefore, does not move out of the inversion symmetric position as the Ti^{4+} does. Fe^{3+} is passive and does not take part in the phase transitions as Ti^{4+} does. *However, it sees the near intrinsic oxygen surroundings and therefore is a very useful probe about the bulk oxygen lattice alone.* This behavior of Fe^{3+} in $BaTiO_3$ is not a single example, but rather appears to be a general feature in ferroelectric oxide perovskites as our results in $PbTiO_3$

TABLE IV. Comparison of experimental Mn^{2+} data with three different models on the basis of the superposition model.

	Mn^{2+} in tetragonal $BaTiO_3$	Mn^{2+} in tetragonal $PbTiO_3$
Superposition-model data	$R_0 = \frac{1}{2}c = 2018$ Å $\bar{b}_2(R_0) = -0.208(16)$ (cm^{-1}) $t_2 = 7(1)$	$R_0 = \frac{1}{2}c = 2.076$ Å $\bar{b}_2(R_0) = -0.171(9)$ (cm^{-1}) $t_2 = 7(1)$
Experimental EPR data	$b_2^0 = +215(2) \times 10^{-4}\ \text{cm}^{-1}$ at $T = 300$ K, Ref. 20	$b_2^0 = +502(4) \times 10^{-4}\ \text{cm}^{-1}$ at $T = 300$ K, Ref. 21
Ti coordinate model	$b_2^0 = -550(220) \times 10^{-4}\ \text{cm}^{-1}$	$b_2^0 = -1223(550) \times 10^{-4}\ \text{cm}^{-1}$
Centered model	$b_2^0 = +333(76) \times 10^{-4}\ \text{cm}^{-1}$	$b_2^0 = +1844(433) \times 10^{-4}\ \text{cm}^{-1}$
One-parameter model dislocation Δ to obtain the experimental b_2^0 value	$\Delta = -0.024(2)$ $D = \Delta \times c = -0.10$ Å	$\Delta = +0.023(1)$ $D = \Delta \times c = +0.10$ Å

and $KNbO_3$ indicate. The larger Mn^{2+} behaves in a similar but not identical manner.

The distortion of the oxygen octahedron about the inversion symmetric coordinate is proportional to the lattice strain. The latter in turn depends quadratically on the polarization $P(T)$ in the tetragonal phase, as the crystal is only electrostrictive in the cubic phase.[2] This explains, in agreement with earlier work, the relation $b_2^0(T) = 1.40[P(T)]^2$ observed. In the latter relation, P is measured in μ/cm^2 and b_2^0 in 10^{-4} cm^{-1}. Wemple[23] calculated the axial b_2^0 parameter in the presence of a lattice polarization P_s assuming it results entirely from lattice strain $\epsilon \simeq 10^{-3}P_s^2$ (ϵ in percent). Then using the measured proportionality of $D = b_2^0$ with strain $D = 0.14\epsilon(cm^{-1})$ for Fe^{3+} in MgO he obtained $D = 1.4P_s^2$. Our findings justify why his calculation was successful: the Fe^{3+} in MgO is centered in the octahedron, as well as in ferroelectric $BaTiO_3$, whether the octahedron is strained by direct uniaxial stress or by a given polarization through electrostrictive strain.

Sakudo[3] discussed his results in terms of a model of consecutive ordering of *oxygen* polarizations along [100] (tetragonal phase), [100] and [010] (orthorhombic phase), and finally [100], [010], and [001] (rhombohedral phase) directions. He then expressed doubts about his interpretations, because in the NMR results of $KNbO_3$, an orthorhombic nuclear quadrupole splitting of the Nb nucleus was observed in the orthorhombic phase.[24] In the light of our findings, the difference in behavior is obvious as the Nb is at the intrinsic displaced lattice coordinate and the Fe^{3+} is not. The reason why this was not recognized is that, at the time, one was not aware of the sensitivity of the EPR and NMR to inner electric fields and covalency: the success of the present work underlines that the EPR b_2^m parameters are determined, to a large extent, by the next-neighbor ligand positions. In contrast, the nuclear quadrupole splitting is proportional to the second derivative of the crystal field. The latter is a slowly converging function of summations of individual monopole, dipole, and quadrupole contributions.[25] Thus, NMR and EPR do not measure the same property even if the probing Fe^{3+} ion is located at the exact Ti^{4+} site.

The Sakudo model of consecutive ordering of oxygen polarizations along the three independent ⟨100⟩ directions has, according to our work, to be replaced by the ordering of local oxygen "position". Our model is also in agreement with the analysis of the EPR $BaTiO_3$:Gd^{3+} results by Takeda[5]: He computed the electric field gradients on the Ba^{2+} (Gd^{3+}) site resulting from the nearest-intrinsic-neighbor oxygen positions including their polarization and the contributions from Ti^{4+} ions. He obtained reasonable agreement in assuming oxygen polarizations parallel to the ⟨110⟩ and ⟨111⟩ directions, respectively, thus ruling out the ⟨100⟩ parallel polarization models in the orthorhombic and rhombohedral phases. As in our application of the Newman superposition model the *oxygen positions* only determine the crystal-field splitting of the Fe^{3+} level, our findings are in agreement with the Gd^{3+} data.

Our microscopic findings on the local position of the Fe^{3+} in $BaTiO_3$ is also of value to understand the shift in T_c upon iron doping. The spontaneous polarization of the ferroelectric $BaTiO_3$ stems mainly from the shift of the Ti^{4+} ions from the center of the oxygen octahedra. In Fe^{3+}-doped $BaTiO_3$, the local polarization in a $Fe^{3+}O_6$ cluster is zero because Fe^{3+} is in the center of the octahedron. Therefore, the polarization of the entire material is reduced proportionally to the concentration of the doping. The dipole-dipole interaction between the permanent dipoles is also partly blocked, and the region of correlation will be smaller than in undoped material. T_c will therefore be reduced by doping with Fe^{3+}. This characteristic behavior was observed by Arend[26] and more recently by Ihrig[27] for the cubic-to-tetragonal phase transition of $BaTiO_3$.

Sakudo[3] and Sakudo and Unoki[4] found that the cubic parameter a is within 10% insensitive to the phase transitions. From our calculation, we came to the conclusion that the origin of the constants of the cubic parameter a lies in similar surroundings in all phases of $BaTiO_3$. Because Fe^{3+} is in the center of the octahedron, the distances in all four phases to the oxygens and the covalency are about the same, and, therefore, the cubic parameter a is about the same. Its small amount in $BaTiO_3$ and $KNbO_3$ has been noted by Müller[28] and will be discussed elsewhere[29] in relation to recent theories of ferroelectricity.[30]

Finally, we wish to give a qualitative idea why Fe^{3+} behaves differently from Ti^{4+}. This can be done with arguments from the lattice-dynamical theory.[31] In displacive structural phase transitions such as in $BaTiO_3$, the ferroelectric transition has its origin in a cancellation of the positive short-range interaction by the negative Coulomb interaction. The frequency of the soft mode, ω_0, is given by

$$\mu\omega_0^2 \propto S - C \quad , \tag{4}$$

where μ is a reduced mass, S is the short-range interaction, and C is the Coulomb interaction. $BaTiO_3$ undergoes a ferroelectric transition at T_c; therefore the amount of the short-range interaction is identical to the Coulomb interaction. In the $Ti^{4+}O_6$ cluster, this behavior is observed but not in the $Fe^{3+}O_6$ cluster, as shown by our model calculation. The differences in this behavior must have their origin in differences between Ti^{4+} and Fe^{3+}. They have different masses [$m(Ti^{4+}) = 47.9$; $m(Fe^{3+}) = 55.8$],

but as Eq. (4) shows, only a proportional factor is changed. They have about the same ionic radii[22] [$r(Fe^{3+}) = 0.64$ Å and $r(Ti^{4+}) = 0.60$ Å; 0.68 Å (Ahrens)]. There is, however, a nominal difference in the charge. The Fe^{3+} ion has three and the Ti^{4+} four positive charges. However, the effective charges of both are considerably lower; with the Ti^{4+} still a fraction of e higher than that of the Fe^{3+}. Whether this small difference is sufficient to yield cancellation of forces for the Ti^{4+} but not for the Fe^{3+} is doubtful. Consider the Sn^{4+} at an octahedral site which suppresses the transition ($BaSnO_3$ is not ferroelectric)[32] and certainly has a higher effective charge than the Fe^{3+} with almost the same ionic radius. What Sn^{4+} and Fe^{3+} have and the Ti^{4+} or Nb^{5+} do not is the following: the Fe^{3+} has a half-filled $3d$ shell, $3d^5$, and the Sn^{4+} has a completely filled $4d$ shell, $4d^{10}$, i.e., their anti- and nonbonding d orbitals are half or totally occupied.[33] Both ions suppress the ferroelectric transition. Thus the unfilled d shells of Ti^{4+} and Nb^{5+} appear to be crucial to the existence of ferroelectricity with displaced B ions, apart from the anisotropic nonlinear polarizability of the oxygens (absent for S^{2-}, F^-, Cl^-, etc.). The latter was shown to be of importance by the microscopic theory of Migoni *et al.*[30] due to the volume dependence of the oxygen p electrons. If the latter p-electron charge can move onto empty d-cation orbits, the oxygen shell polarizability is enhanced and ferroelectricity occurs. Here we have certain evidence that a half-occupied d shell is sufficient to inhibit the effect.

VI. CONCLUSIONS

We have shown quantitatively that the Fe^{3+} in $BaTiO_3$ as well as in $KNbO_3$ and $PbTiO_3$ remains at the center of the octahedrons in their ferroelectric phases, where the Ti and Nb ions are off-center. Our results are in agreement with all previously reported EPR data and latest intrinsic x-ray refined structure analysis. The "inertness" of the Fe^{3+} to off-center motion is suggested to be due to its half-filled $3d^5$ shell in contrast to the unfilled d shells of Ti^{4+} or Nb^{5+}, all ions having almost the same size.

The superposition model has proven to be a really valid tool to obtain our quantitative results. They show that the Fe^{3+} is a sensitive probe for the intrinsic distortion of the oxygen octahedron surrounding it. The crucial probing difference between local short-range nearest-neighbor positions detected by EPR and local long-range crystal fields in NMR has been emphasized.

ACKNOWLEDGMENTS

The authors wish to thank Dr. R. Schollmayer and Dr. W. Schildkamp of the University of Saarbrücken, West Germany, for obtaining the crystallographic data of the tetragonal and rhombohedral phases of $BaTiO_2$ prior to publication. One of us (E.S.) is also indebted to Professor W. Urban and Professor D. J. Newman for stimulating discussions. The calculations were done on the IBM 370/168 computer of the RHRZ Bonn.

[1] A. W. Hornig, R. C. Rempel, and H. E. Weaver, J. Phys. Chem. Solids 10, 1 (1959).
[2] L. Rimai and G. de Mars, Phys. Rev. 127, 702 (1962).
[3] T. Sakudo, J. Phys. Soc. Jpn. 18, 1626 (1963).
[4] T. Sakudo and H. Unoki, J. Phys. Soc. Jpn. 19, 2109 (1964).
[5] T. Takeda, J. Phys. Soc. Jpn. 24, 533 (1968).
[6] D. J. Newman, Adv. Phys. 20, 197 (1971).
[7] D. J. Newman and W. Urban, Adv. Phys. 24, 793 (1975).
[8] E. Siegel and K. A. Müller, Phys. Rev. B 19, 109 (1979).
[9] K. A. Müller, Ferroelectrics 13, 381 (1976).
[10] D. J. Newman and E. Siegel, J. Phys. C 9, 4285 (1976).
[11] *Landolt Börnstein: Numerical Data and Fundamental Relationships in Science and Technology* (Springer, Berlin, 1969), Vol. 3, p. 51.
[12] R. Shollmayer (private communication).
[13] G. Shirane, H. Danner, and R. Pepinsky, Phys. Rev. 105, 856 (1957).
[14] W. Schildkamp (private communication).
[15] J. Y. Buzaré, Ph.D. thesis (L'Université Le Mans, France, 1978) (unpublished).
[16] G. Shirane, R. Pepinsky, and B. C. Frazer, Acta Crystallogr. 9, 131 (1956).
[17] R. G. Pontin, E. F. Slade, and D. J. E. Ingram, J. Phys. C 2, 1146 (1969).
[18] A. W. Hewat, J. Phys. C 6, 2559 (1973).
[19] E. Siegel, W. Urban, K. A. Müller, and E. Wiesendanger, Phys. Lett. A 53, 415 (1975).
[20] H. Jkushima, J. Phys. Soc. Jpn. 21, 1866 (1966).
[21] H. Jkushima and S. Hayakawa, J. Phys. Soc. Jpn. 27, 414 (1969).
[22] H. D. Megaw, *Crystal Structure: A Working Approach* (Saunders, Philadelphia, 1973), p. 26.
[23] S. H. Wemple, MIT Technical Report No. 425 (unpublished).
[24] R. M. Cotts and W. D. Knight, Phys. Rev. 96, 1285 (1954).
[25] A. Avogadro, G. Bonera, F. Borsa, and A. Rigamonti, Phys. Rev. B 9, 3905 (1974).
[26] H. Arend, in *Proceedings of the International Meeting on Ferroelectricity,* edited by V. Dvorak, A. Fouskova, and P. Glogar (Institute of Physics of the Czechoslovak Academy of Sciences, Prague, 1966), p. 231.
[27] H. Ihrig, J. Phys. C 11, 819 (1978).
[28] K. A. Müller, Phys. Rev. B 13, 3209 (1976).
[29] K. A. Müller and Th. von Waldkirch (unpublished).
[30] R. Migoni, H. Bilz, and D. Bäuerle, Phys. Rev. Lett. 37, 1155 (1976).
[31] G. Samara, Comments Solid State Phys. 8, 13 (1977).
[32] F. Jona and G. Shirane, *Ferroelectric Crystals* (Pergamon, London, 1962), p. 249.
[33] The Zr^{4+} also suppresses the ferroelectric $BaTiO_3$ transi-

tion (Ref. 32) despite its having an empty $4d$ shell, but its ionic radius is $r = 0.78$ Å as compared to the $r = 0.68$ of Ti^{4+}, i.e., the Zr^{4+} cannot move off-center by 0.1 Å and we have a size effect. Actually, Zr^{4+} suppresses T_c about half as much as Sn^{4+} with a full $4d^{10}$ shell and a radius of $r = 0.71$ Å, which is near that of Ti^{4+}. This shows that in Sn^{4+} it is the full $4d^{10}$ shell which leads to the suppression, whereas in the larger Zr^{4+} the empty $4d^0$ shell, which is favorable for ferroelectricity, *counteracts* the suppressive effect of its large size.